# Three-Dimensional Visualization of a Human Chromosome Using Coherent X-Ray Diffraction

Yoshinori Nishino,[1,*] Yukio Takahashi,[2] Naoko Imamoto,[3] Tetsuya Ishikawa,[1] and Kazuhiro Maeshima[3]

[1]*RIKEN SPring-8 Center, 1-1-1 Kouto, Sayo-cho, Sayo-gun, Hyogo 679-5148, Japan*
[2]*Graduate School of Engineering, Osaka University, 2-1 Yamada-oka, Suita, Osaka 565-0871, Japan*
[3]*Cellular Dynamics Laboratory, RIKEN, 2-1 Hirosawa, Wako, Saitama 351-0198, Japan*

(Received 10 July 2008; revised manuscript received 18 November 2008; published 5 January 2009)

Coherent x-ray diffraction microscopy is a lensless phase-contrast imaging technique with high image contrast. Although electron tomography allows intensive study of the three-dimensional structure of cellular organelles, it has inherent difficulty with thick objects. X rays have the unique benefit of allowing noninvasive analysis of thicker objects and high spatial resolution. We observed an unstained human chromosome using coherent x-ray diffraction. The reconstructed images in two or three dimensions show an axial structure, which has not been observed under unstained conditions.

DOI: 10.1103/PhysRevLett.102.018101 PACS numbers: 87.59.−e, 42.30.Wb, 61.05.cp, 87.16.Sr

Mesoscopic-scale structures, such as higher-order structures in cellular organelles, play a key role in elucidating the connection between macroscopic properties and atomic structures, but are often too thick to observe under a transmission electron microscope [1,2]. X rays can be used to observe internal mesoscopic structures owing to their short wavelength and high penetrating power [3–6].

Coherent x-ray diffraction occurs when a sample is illuminated by x rays with a well-defined wave front, and its high sensitivity to the sample structure can be utilized for microscopy [7–9]. The coherent diffraction pattern is speckled when the sample is disordered. In an experiment, the speckled diffraction pattern has to be sampled finely enough to satisfy the oversampling condition, which is derived from the Shannon sampling theorem, as Sayre originally pointed out in 1952 [7]. The coherently diffracted wave is related to the sample electron-density map by Fourier transform, but the phase of the diffracted wave is not directly measurable. In x-ray diffraction microscopy, a sample image is reconstructed by retrieving the phase using an iterative method [10]. Coherent diffraction in the hard x-ray regime can provide three-dimensional (3D) electron-density maps, a seamless connection with x-ray crystallography. Despite strong interest in biological applications, biological studies have been limited to two-dimensional (2D) observations [11–14]. We report for the first time 3D electron-density mapping of an uncrystallized biological sample using coherent x-ray diffraction.

Coherent x-ray diffraction microscopy is an ideal form of x-ray phase-contrast imaging, since there is no contrast degradation due to lenses. Meanwhile, conventional soft x-ray zone plate microscopes and x-ray contact microscopes provide absorption contrast [3–5]. As is well recognized in optical microscopy, phase-contrast imaging generally offers better image contrast than absorption contrast imaging for transparent objects, such as unstained biological specimens. In the x-ray regime also, it has been reported that lower radiation dose and higher image contrast can be achieved with phase-contrast imaging compared to absorption contrast imaging, even in the water window region [15]. The reconstructed images of an unstained human chromosome shown in this Letter have axial structure, which other microscopic methods have been unable to visualize under unstained conditions, and the result experimentally demonstrates the high imaging ability of coherent x-ray diffraction for unstained biological specimens.

Chromosomes are essential organelles for the faithful transmission of duplicated genomic DNA into two daughter cells during cell division [16,17]. Although more than 100 years have passed since chromosomes were first observed, how a long string of genomic DNA is packaged into compact chromosomes remains unclear. Since whole-mount chromosomes are too thick for electrons, thin-sectioning is unavoidable in transmission electron microscopy; however, it generally requires sample preparation and often causes deformation of the sections [1]. Although light microscopy with immunofluorescence or fluorescent proteins can image whole-mount chromosomes, the distribution of specific proteins only can be observed, requiring *a priori* knowledge or conjecture about the sample. Therefore, x rays have a unique potential for analyzing the entire structure of whole-mount chromosomes.

We purified individual chromosomes from mitotic HeLa cells as described previously [18]. The chromosomes were fixed chemically in a compact form with a buffer including 10 mM Hepes-KOH, 5 mM $MgCl_2$ and 0.5% glutaraldehyde for 10 min. The fixed chromosomes were spread over a 100-nm-thick silicon nitride membrane by gentle centrifugation to adhere the chromosomes to the membrane at an appropriate density. The chemically fixed chromosomes on the silicon nitride membrane were washed once with pure distilled water to remove salt and then allowed to dry in air.

We observed a human chromosome sample under our coherent x-ray diffraction microscope using the BL29XUL hard x-ray undulator beam line at SPring-8. Figure 1 shows the experimental setup schematically. X rays at an energy of 5 keV pass through a 20-$\mu$m-diameter pinhole to illu-

 

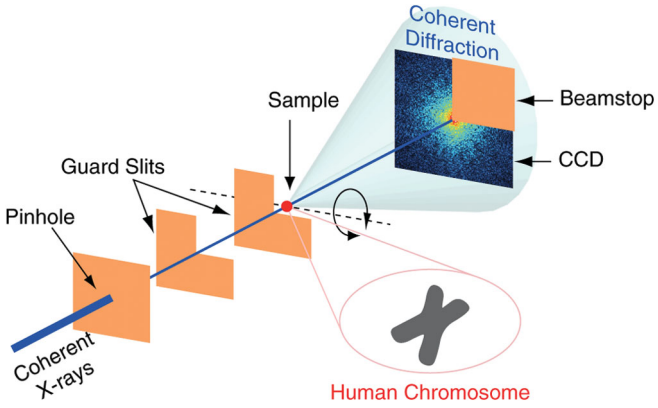


FIG. 1 (color). Schematic view of coherent hard x-ray diffraction measurement of an unstained human chromosome. A 20-$\mu$m-diameter pinhole ~1 m upstream from the sample defined the illumination for a single chromosome. Two guard slits were aligned carefully to reduce the amount of missing data near forward-scattering angles. An x-ray CCD detector 1.32 m downstream from the sample was used to acquire coherent diffraction data. The CCD has a pixel size of 20 $\mu$m, and an imaging array of 1340 × 1300 pixels. A beam stop 365 mm upstream from the CCD blocked the unscattered direct x-ray beam, and shaded nearly a quadrant area of the CCD. The centrosymmetry of the diffraction data was used to recover some of the missing data behind the beam stop. The sample was rotated for 3D image reconstruction.

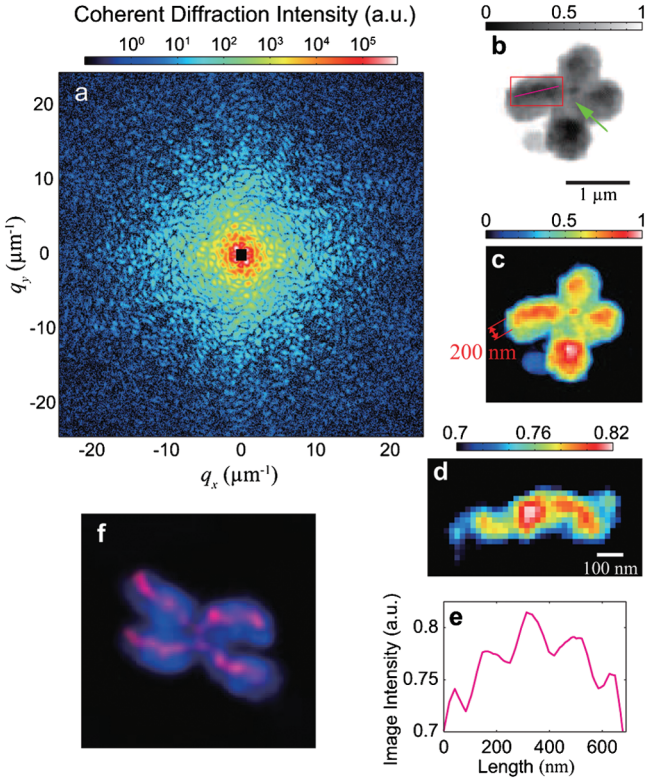


FIG. 2 (color). Coherent diffraction pattern of an unstained human chromosome and its reconstructed projection image. The reconstruction of coherent x-ray diffraction data (a) gave a chromosome image [(b) in gray scale and (c) in color scale]. The centromere region is indicated by an arrow in (b). The reconstructed image contains a high-intensity region resembling the chromosome axial structure near the center of the chromatids, as clearly shown in (c). (d) shows an enlarged image of the region in the red square in (b), where a different color scale was used to enhance the structure. A wavy feature in (d) is similar to the helical axis structure observed in the immunofluorescence imaging [18]. The wavy structure is also evident in the profile (e) along the magenta line in (b). (f) shows an immunofluorescence image of a different chromosome, stained by a condensin antibody (red) and DAPI (blue), showing a wavy axial structure (red). $\boldsymbol{q}$ is defined as $|\boldsymbol{q}| = 2\sin(\Theta/2)/\lambda$, where $\Theta$ is the scattering angle.

minate the target chromosome only. The photon flux after the pinhole was ~$1 \times 10^{10}$ photons/s. The beam size at the sample (the size of the first robe of the pinhole diffraction) is calculated to be 33 $\mu$m. Our measurement is insensitive to the positional drift of the sample, because the illuminating beam size is an order of magnitude larger than the sample size, and there is no neighboring object near the sample chromosome. The coherent diffraction from the sample is recorded with an x-ray direct-detection charge-coupled device (CCD). In the data analysis, we used 800 × 800 pixel data, which provided reconstructed images with a single pixel (or a voxel) size of 20.5 nm in each dimension. For 3D reconstruction, we measured data at different incident angles ranging from −70° to +70° at intervals of 2.5° or 5°. In the data analysis, we excluded data at some angles suffering from strong background scattering. The exposure time at each incident angle was 2700 s for the sample data (except for the data shown in Fig. 2, which had a 3400 s exposure) and half of that for the background data. The radiation dose was $4 \times 10^8$ Gy for a single incident angle and $2 \times 10^{10}$ Gy for full 3D data acquisition.

Our coherent diffraction measurement produced high-contrast speckle patterns, as shown in Fig. 2(a), though the sample human chromosome was not stained. Speckles in the coherent diffraction patterns have a typical size of ~8 pixels on the detector in each dimension; therefore, our measurement safely satisfies the oversampling condition. We achieved a typical missing data size of 23 pixels near the diffraction center.

We reconstructed an image from the coherent diffraction data by applying an iterative phasing method [10,19,20]. Specifically, we used the HIO algorithm [10] with the iterative normalization [19]. The iterative process started from a random electron-density map in a rectangular support (99 × 98 pixels), and the support was revised iteratively [20] every 500 iterations using intermediately reconstructed images. Here, the support is the area where the sample is supposed to exist. In the iterative process, the electron density outside the support is forced to decrease gradually in real space, and the measured coherent diffraction data is used in reciprocal space. The iterative process

continued for up to $2 \times 10^4$ iterations. Images were reconstructed starting from 15 different random electron-density maps, and the ten most similar resultant images were averaged after careful alignment to achieve the final reconstruction. The similarity evaluation and the alignment were performed numerically by comparing digital images.

A 2D reconstruction of the human chromosome is shown in gray scale [Fig. 2(b)] and in color scale [Fig. 2(c)]. In these figures, the image intensities are proportional to the projection of the electron density in the direction of the incident x-ray beam. According to our estimation using the phase retrieval transfer function [21], the spatial resolution (half-period resolution) of the 2D reconstruction is 38 nm. This implies that the Fourier transform of the reconstructed image is highly consistent with the measured coherent diffraction data below the resolution frequency.

The 2D projection image [Figs. 2(b) and 2(c)] clearly shows a pair of sister chromatids attached to each other at the centromere region [indicated by an arrow in Fig. 2(b)]. We even observed a protrusion from the bottom arm of the chromosome in lower image intensities; this is likely part of another chromosome that failed to separate during sample preparation. The most striking feature in the 2D reconstruction is the high image-intensity region near the center of the chromatids, which is obvious in the color scale image [Fig. 2(c)]. The high image-intensity region has a width of ~200 nm, and the intensity is typically ~1.5 times greater than in the other region. This region roughly coincides with where the so-called chromosome scaffold or axis appears. The axis was reported to consist of condensin and topoisomerase II$\alpha$, which are essential proteins for the chromosome assembly process [16–18]. The axial structure has so far been detected only using immunoelectron microscopy or fluorescence microscopy on labeling its components, which have a diameter of ~200 nm at the center of each chromatid in isolated chromosomes and even in chromosomes in living cells [16,17]. The corresponding region in our reconstruction has a wavy structure, as shown in the enlarged image in Fig. 2(d). This wavy feature is similar to the helical structure in the chromosome, as observed with immunofluorescence imaging [18], but has not been seen in unstained chromosomes. Figure 2(f) shows an immunofluorescence imaging of a different chromosome, showing an axial structure (red) in the chromosome body (blue).

A greater image intensity in 2D projection images implies a greater electron density or a thicker sample depth, and a 3D reconstruction allows us further interpretation. For 3D data analysis, we used coherent diffraction data sets at 38 incident angles, and performed image reconstruction in a similar way as in the 2D case but using 3D Fourier transformation. The diffraction intensity in each voxel was obtained from the measured coherent diffraction data sets by interpolation [22]. Prior to the interpolation, each diffraction data set was normalized using the total number of electrons in the 2D reconstruction at each incident angle. The iterative process continued for up to $1 \times 10^4$ iterations for the 3D case, and the final averaging process was applied as in the 2D case.

Figure 3 shows our 3D reconstruction. It shows not only the surface morphology [Fig. 3(a)], but also the internal electron-density map [Figs. 3(b), 3(c), and 3(e)]. Interestingly, we found the greatest electron density around the centromere (indicated by arrows). Figures 3(b) and 3(c) show cross-sectional images through the highest density position in the horizontal and vertical planes, respectively. Our observation can be explained by the fact that the centromere region is composed entirely of constitutive heterochromatin and is more condensed than other chromosomal regions. In the projection image [Fig. 3(d)] generated from the 3D reconstruction, the greatest image intensity appears at the bottom arm of the chromosome which is consistent with our 2D reconstruction [Figs. 2(b) and 2(c)].

Near the central axis of each chromatid, the electron density is also relatively high [Figs. 3(b), 3(c), and 3(e)]. This result indicates that the axial region has a greater electron density than the average, at least in this sample, and again suggests the region is more condensed. The wavy structure observed in the 2D reconstruction was not recognized in the 3D case, since the spatial resolution was

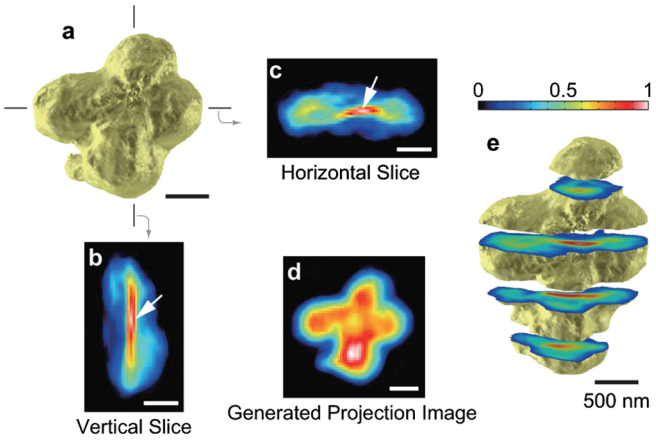


FIG. 3 (color). Reconstructed 3D electron-density map of an unstained human chromosome. The isosurface (a) of the chromosome was drawn with a threshold value at 15% of the highest density. The planes of the cross-sectional images (b,c) include the position near the centromere (indicated by arrows) with the highest electron density. They show relatively high density near the central axis of each chromatid. The projection image (d) generated from the 3D reconstruction has a similar feature to that in the 2D reconstruction in Figs. 2(b) and 2(c). (e) shows cross-sectional images of the chromosome at 409 nm intervals. The diffraction data sets used for the 3D analysis are at 38 incident angles: every 2.5° from −70° to −27.5°, as well as −7.5°, −5°, 0°, 5°, 7.5°, 10°, 15°, 17.5°, 20°, 25°, 27.5°, 30°, 37.5°, 40°, 45°, 47.5°, 50°, 55°, 57.5°, and 60°.

lower. We estimate the spatial resolution of the 3D reconstruction to be 120 nm from the phase retrieval transfer function [21]. Nevertheless, this is amongst the highest resolutions ever achieved for 3D x-ray phase-contrast imaging [23,24]. The result also implies that our microscope detects the phase shift of x-ray waves with great sensitivity. Judging from the radiation dose of our measurement, $2 \times 10^{10}$ Gy, and the reported feature-destroying dose [25,26], the resolution degradation in the 3D case is caused primarily by radiation damage. For organic samples, mass loss due to outgassing occurs after radiation-induced bond braking, and causes morphological change [3]. Higher resolution is expected to be achieved by carefully optimizing the radiation dose in consideration of the dose fractionation theorem [27] and by cryogenically cooling the sample. Note that we succeeded in reconstructing 3D images, even when radiation damage presumably develops over the measurement time. A similar phenomenon would also be seen in any tomographic imaging.

Our findings give clear guidelines for the 3D structure analysis of thick unstained biological samples using hard x rays, and our method was shown to provide structural information that complements conventional imaging methods experimentally. This was realized as a consequence of our high-quality data acquisition of coherent diffraction. Our method eliminates the shortcomings of hard x-ray microscopy using lenses, realizing an ideal form of lensless phase-contrast hard x-ray imaging. As Henderson discussed after considering the electron mean free path, x rays can offer a superior performance compared to the electrons for biological samples thicker than $\sim$500 nm [2]. Since our sample was dried, measurement in a hydrated state is the ultimate goal for observing samples closer to their natural state. In the measurement of frozen-hydrated biological samples, where vitreous ice is widely spread, coherent diffraction measurement with scanning of the finite illumination area (ptychography) will be beneficial [28,29], though the extension to the 3D observation is not straightforward.

In x-ray diffraction microscopy using synchrotron radiation, the spatial resolution is often limited by the radiation damage [2] and/or by the statistical precision of the coherent diffraction data at high angles. The limitations will be removed or lowered dramatically with the x-ray free electron lasers (XFELs) currently being developed. The radiation damage can be reduced considerably by taking data before the sample is destroyed [21,30]. In such experiments, the stereo-3D imaging can be used to obtain 3D structural information [31]. Higher statistical precision can be obtained by focusing the XFEL beam to match the sample size [32,33]. We estimate from a simple flux calculation that a single focused XFEL pulse is enough for 2D reconstruction of a micrometer-sized sample by producing the coherent diffraction data at similar statistical accuracy to the present data, which currently takes about one hour to record.

Y. N. thanks A. Ito and K. Shinohara for the discussion on dose estimation. We thank K. Namba, J. Mizuki, T. Sutani and M. Nakasako for critical reading of the manuscript. This study was supported by KAKENHI, the Promotion of XFEL Research of MEXT, and a grant on Advanced Medical Technology from MHLW.

*nishino@spring8.or.jp

[1] *Cellular Electron Microscopy, Methods in Cell Biology*, edited by J. R. McIntosh (Academic Press, San Diego, 2007), Vol. 79.
[2] R. Henderson, Q. Rev. Biophys. **28**, 171 (1995).
[3] J. Kirz, C. Jacobsen, and M. Howells, Q. Rev. Biophys. **28**, 33 (1995).
[4] G. Schneider *et al.*, Surf. Rev. Lett. **9**, 177 (2002).
[5] W. Chao, B. D. Harteneck, J. A. Liddle, E. H. Anderson, and D. T. Attwood, Nature (London) **435**, 1210 (2005).
[6] A. Momose, Jpn. J. Appl. Phys. **44**, 6355 (2005).
[7] D. Sayre, Acta Crystallogr. **5**, 843 (1952).
[8] J. Miao, P. Charalambous, J. Kirz, and D. Sayre, Nature (London) **400**, 342 (1999).
[9] M. A. Pfeifer, G. J. Williams, I. A. Vartanyants, R. Harder, and I. K. Robinson, Nature (London) **442**, 63 (2006).
[10] J. R. Fienup, Appl. Opt. **21**, 2758 (1982).
[11] J. Miao, K. O. Hodgson, T. Ishikawa, C. A. Larabell, M. A. Le Gros, and Y. Nishino, Proc. Natl. Acad. Sci. U.S.A. **100**, 110 (2003).
[12] D. Shapiro *et al.*, Proc. Natl. Acad. Sci. U.S.A. **102**, 15 343 (2005).
[13] H. Jiang *et al.*, Phys. Rev. Lett. **100**, 038103 (2008).
[14] C. Song *et al.*, Phys. Rev. Lett. **101**, 158101 (2008).
[15] G. Schneider, Ultramicroscopy **75**, 85 (1998).
[16] J. R. Swedlow and T. Hirano, Mol. Cell **11**, 557 (2003).
[17] K. Maeshima and M. Eltsov, J. Biochem. (Tokyo) **143**, 145 (2008).
[18] K. Maeshima and U. K. Laemmli, Dev. Cell **4**, 467 (2003).
[19] Y. Nishino, J. Miao, and T. Ishikawa, Phys. Rev. B **68**, 220101 (2003).
[20] S. Marchesini *et al.*, Phys. Rev. B **68**, 140101(R) (2003).
[21] H. N. Chapman *et al.*, Nature Phys. **2**, 839 (2006).
[22] J. Miao, T. Ishikawa, B. Johnson, E. H. Anderson, B. Lai, and K. O. Hodgson, Phys. Rev. Lett. **89**, 088303 (2002).
[23] R. Mokso, P. Cloetens, E. Maire, W. Ludwig, and J. Y. Buffiere, Appl. Phys. Lett. **90**, 144104 (2007).
[24] G. C. Yin, F. R. Chen, Y. Hwu, H. P. D. Shieh, and K. S. Liang, Appl. Phys. Lett. **90**, 181118 (2007).
[25] S. Marchesini *et al.*, Opt. Express **11**, 2344 (2003).
[26] M. R. Howells *et al.*, arXiv:physics/0502059.
[27] R. Hegerl and W. Hoppe, Z. Naturforsch. **31A**, 1717 (1976).
[28] J. M. Rodenburg *et al.*, Phys. Rev. Lett. **98**, 034801 (2007).
[29] P. Thibault, M. Dierolf, A. Menzel, O. Bunk, C. David, and F. Pfeiffer, Science **321**, 379 (2008).
[30] R. Neutze *et al.*, Nature (London) **406**, 752 (2000).
[31] D. Sayre, Acta Crystallogr. Sect. A **64**, 33 (2008).
[32] G. J. Williams *et al.*, Phys. Rev. Lett. **97**, 025506 (2006).
[33] C. G. Schroer *et al.*, Phys. Rev. Lett. **101**, 090801 (2008).